**UNIVERSITY OF HELSINKI**

# Limited vertical CO2 transport in stems of mature boreal Pinus sylvestris trees

## Tarvainen, Lasse

2021-01

1    **Limited vertical CO$_2$ transport in stems of mature boreal *Pinus sylvestris* trees**

2    Lasse Tarvainen[1,2,3], Göran Wallin[2], Sune Linder[4], Torgny Näsholm[1], Ram Oren[5,6], Mikaell

3    Ottosson Löfvenius[1], Mats Räntfors[2,†], Pantana Tor-Ngern[7,8], John D. Marshall[1]

4

5    [1]Department of Forest Ecology and Management, Swedish University of Agricultural

6    Sciences (SLU), SE-901 83 Umeå, Sweden

7    [2]Department of Biological and Environmental Sciences, University of Gothenburg, SE-405

8    30 Gothenburg, Sweden

9    [3]Umeå Plant Science Centre, Department of Plant Physiology, Umeå University, SE-901 87

10    Umeå, Sweden

11    [4]Southern Swedish Forest Research Centre, SLU, P.O. Box 49, SE-230 53 Alnarp, Sweden

12    [5]Nicholas School of the Environment & Pratt School of Engineering, Duke University,

13    Durham, NC 27708, USA

14    [6]Department of Forest Sciences, University of Helsinki, FI-00014, Finland

15    [7]Department of Environmental Science, Faculty of Science, Chulalongkorn University,

16    Bangkok, Thailand

17    [8]Environment, Health and Social Data Analytics Research Group, Chulalongkorn University,

18    Bangkok, Thailand

19

20    †Deceased 5th of April 2019

21

24

25    Running head: Limited vertical CO$_2$ transport in Scots pine stems

1
2
3          26
4
5
6          27          Author for correspondence:
7
8          28          Lasse Tarvainen
9
10         29          *Email*: lasse.tarvainen@bioenv.gu.se
11
12         30
13
14
15
16
17
18
19
20
21
22
23
24
25
26
27
28
29
30
31
32
33
34
35
36
37
38
39
40
41
42
43
44
45
46
47
48
49
50
51
52
53
54
55
56
57
58
59
60

31 **Abstract**

32 Several studies have suggested that $CO_2$ transport in the transpiration stream can considerably

33 bias estimates of root and stem respiration in ring-porous and diffuse-porous tree species.

34 Whether this also happens in species with tracheid xylem anatomy and lower sap flow rates,

35 such as conifers, is currently unclear. We infused ^{13}C-labelled solution into the xylem near

36 the base of two 90-year-old *Pinus sylvestris* trees. A custom-built gas exchange system and

37 an online isotopic analyser were used to sample the $CO_2$ efflux and its isotopic composition

38 continuously from four positions along the bole and one upper canopy shoot in each tree.

39 Phloem and needle tissue ^{13}C enrichment was also evaluated at these positions. Most of the

40 ^{13}C label was lost by diffusion within a few meters of the infusion point indicating rapid $CO_2$

41 loss during vertical xylem transport. No ^{13}C enrichment was detected in the upper bole needle

42 tissues. Furthermore, mass balance calculations showed that *c*. 97% of the locally respired

43 $CO_2$ diffused radially to the atmosphere. Our results support the notion that xylem $CO_2$

44 transport is of limited magnitude in conifers. This implies that the concerns that stem

45 transport of $CO_2$ derived from root respiration biases chamber-based estimates of forest

46 carbon cycling may be unwarranted for mature conifer stands.

47

48 Keywords: *[13]C, carbon allocation, pH, respiration, Scots pine, stable isotope, stem $CO_2$*

49 *efflux, xylem transport*

50

**Introduction**

51

52   Several studies have reported that large amounts of carbon dioxide ($CO_2$) can be transported

53   upward by sap flow in the xylem tissues of trees (e.g. McGuire and Teskey 2004, Teskey et

54   al. 2008, Bloemen et al. 2013a, Salomón et al. 2019). Accordingly, it has been shown that up

55   to half of the observed $CO_2$ efflux from tree stems may in fact originate from respiration by

56   other organs or locations, such as roots or stem segments further down the bole, rather than

57   from local sources (Teskey and McGuire 2007). If the net transfer of $CO_2$ by sap flow is

58   away from a given stem segment, chamber-based estimates of the $CO_2$ efflux lead to

59   underestimations of the local respiration rate (e.g. Negisi 1979, Martin et al. 1994, Teskey

60   and McGuire 2007). Furthermore, measurements of foliar photosynthetic efficiency will be

61   biased if xylem-derived $CO_2$ is used as a substrate for carboxylation reactions (Levy et al.

62   1999, McGuire et al. 2009, Bloemen et al. 2013b, Stutz et al. 2017, Stutz and Hanson 2019).

63   Such potential misattributions of the origin of the observed $CO_2$ are major concerns for

64   studies on forest carbon (C) budgets because they suggest that high rates of xylem $CO_2$

65   transport can bias chamber-based estimates of the partitioning between soil and stem

66   respiration, and thus profoundly skew our understanding of ecosystem-scale C cycling (e.g.

67   Aubrey and Teskey 2009, Grossiord et al. 2012, Bloemen et al. 2013a, Etzold et al. 2013).

68        A common technique for evaluating the importance of xylem $CO_2$ transport is to assess

69   the $CO_2$ budget of a given stem segment using the mass balance approach (McGuire and

70   Teskey 2004, Bowman et al. 2005, Salomón et al. 2018). According to this approach, the

71   total $CO_2$ efflux from a stem segment is determined by: i) the transport rate of $CO_2$ and its

72   equilibrium species ($H_2CO_3$, $HCO_3^-$ and $CO_3^{2-}$), hereafter collectively called "dissolved $CO_2$"

73   ($CO_2^*$), in the xylem, which in turn depends on the flow rate, the pH and the temperature of

74   the xylem sap, ii) the often strongly temperature-dependent local respiration rate, and iii) the

75   change in mean sap $CO_2$ concentration [$CO_2$] over time (i.e. change in storage within the

1
2
3
4
5
6
7
8
9
10
11
12
13
14
15
16
17
18
19
20
21
22
23
24
25
26
27
28
29
30
31
32
33
34
35
36
37
38
39
40
41
42
43
44
45
46
47
48
49
50
51
52
53
54
55
56
57
58
59
60

76    segment). Notably, the net efflux may also be reduced by corticular photosynthesis resulting

77    in refixation of some portion of the outward diffusing $CO_2$ (e.g. Pfanz et al. 2002, Wittmann

78    et al. 2006, Tarvainen et al. 2018). However, corticular photosynthesis is not included in the

79    commonly used formulation of the mass balance equation for assessing stem $CO_2$ fluxes

80    (McGuire and Teskey 2004) because most studies have used opaque chambers. In addition, it

81    has been recently suggested that the ratio of $CO_2$ efflux to $O_2$ influx (ARQ, apparent

82    respiratory quotient) can be used to make inferences of the fate of the $CO_2$ in stems (Angert

83    et al. 2012, Hilman and Angert 2016, Hilman et al. 2019). Because the main respiratory

84    substrate in stems is believed to be carbohydrates (Hoch et al. 2003, Plaxton and Podestá

85    2006), ARQ values < 1.0, reported for several species, indicate that respired $CO_2$ is retained

86    in the stem (Angert et al. 2012, Hilman et al. 2019). The low ARQ values were originally

87    interpreted as evidence of $CO_2$ transport in xylem sap flow away from the respiring tissues

88    (Angert et al. 2012). However, it was recently shown that ARQ is independent of sap flow

89    rate, leading to a suggestion that the low ARQ values are instead caused by refixation of

90    respired $CO_2$ by local biosynthesis reactions (Hilman et al. 2019) e.g. by the enzyme

91    phosphoenolpyruvate carboxylase (PEPC) that is known to be present in tree stems

92    (Berveiller and Damesin 2008).

93      The evaluation of the ecological significance of xylem $CO_2$* transport is further

94    complicated by the fact that the factors controlling stem C cycling may exhibit considerable

95    variation among geographic locations, tree species, and seasons. In general, studies showing

96    high rates of xylem $CO_2$* transport have been carried out in species with small conducting

97    areas and high sap flow rates (Ubierna et al. 2009), although xylem $CO_2$* transport was found

98    to increase with stem size and sapwood conducting area in *Liriodendron tulipifera* L. (yellow

99    poplar) (Fan et al. 2017). In contrast, transport rates have been suggested to be generally low

100    in species with tracheid anatomy, such as conifers (Maier and Clinton 2006, Ubierna et al.

101   2009, Powers and Marshall 2011). However, methodological concerns have been raised

102   regarding these earlier conifer studies (see below). A specific challenge for using the mass

103   balance approach for conifers is that resin production hinders the use of $CO_2$ probes. In

104   addition, reduced rates of stem $CO_2$ efflux have been reported also in conifers during periods

105   of high transpiration and attributed to increased $CO_2$* transport in the xylem (e.g. Martin et

106   al. 1994, Bowman et al. 2005).

107        The mass balance approach can be used to quantify the overall net $CO_2$ transport

108   through a given stem segment, but it cannot tell us what happens to the transported $CO_2$ on

109   the whole tree-scale. More detailed analyses of where the transported $CO_2$ ends up have been

110   made by introducing isotopically labelled C in the xylem and following its accumulation in

111   plant tissues. However, the efflux of the labelled C from the bole and the branches is

112   generally not measured in these studies; rather it is assumed that any label not recovered in

113   the tissues has been lost to radial diffusion. Such studies on conifers have suggested that the

114   importance of transported C for the overall C gain of seedlings (Ford et al. 2007) and for the

115   stem $CO_2$ efflux of large trees (Ubierna et al. 2009) is small. Notably, the label solution in

116   these previous studies was applied to the soil rather than directly into the xylem, and hence it

117   has been suggested that these experiments do not accurately depict the transport of $CO_2$

118   derived internally from root respiration (Bloemen et al. 2013a). Powers and Marshall (2011)

119   carried out an *in situ* xylem labelling of a field-grown *Thuja occidentalis* L. (northern white

120   cedar) tree and found no evidence of the label reaching the top of the canopy foliage. In

121   contrast, Bloemen et al. (2013a) made a comprehensive analysis of the fate of xylem $CO_2$ in

122   seven-year-old *Populus deltoides* Barts. Ex Marsh (eastern cottonwood) trees using a similar

123   labelling approach as Powers and Marshall (2011) and by collecting tissue samples from

124   different parts of the tree. They detected considerable ^{13}C enrichment in sampled organs

125    (stems, branches and leaves) throughout the canopy and concluded that xylem transport was

126    an important mechanism for internal C cycling in trees.

127        Thus, there is a disagreement regarding the importance of xylem $CO_2$ transport between

128    studies made on conifers *vs*. diffuse-porous or ring-porous species (Ubierna et al. 2009,

129    Trumbore et al. 2013) and to some extent between different experimental approaches. In the

130    current study, our aim was to investigate in detail the xylem transport of $CO_2$ in large conifer

131    trees growing in the field. To this end we carried out a $^{13}C$ tracer experiment that utilised an

132    experimental setup that enabled us to monitor the dynamics of tracer movement over an

133    extended period of time. The setup consisted of a custom-built gas exchange system (Wallin

134    et al. 2001) combined with a Picarro cavity ring-down spectrophotometer (CRDS) to

135    continuously measure the stem $CO_2$ efflux and its isotopic composition at several positions

136    along the bole, and the top of the canopy shoots, of mature boreal *Pinus sylvestris* L. (Scots

137    pine) trees. Salomón et al. (2019) recently described an analogous approach utilising the

138    CRDS technology and isotopic labeling for measuring the xylem transport of $CO_2$ in four-

139    year-old glasshouse-grown *Populus tremula* L. (European aspen) trees. They suggested that

140    the approach had "outstanding" potential for advancing the understanding of $CO_2$ movement

141    is stems and the respiratory physiology in woody tissues. Based on the earlier work on

142    conifers (e.g. Ford et al. 2007, Ubierna et al. 2009, Powers and Marshall 2011, Tarvainen et

143    al. 2014, 2018) we hypothesised that i) the xylem $CO_2$ transport is of limited magnitude in

144    mature conifers, and subsequently that ii) the stem $CO_2$ efflux from a given bole segment is

145    dominated by locally respired $CO_2$.

146

147

148

149

150    **Material and Methods**

151    *Sample trees and site conditions*

152    The movement of the $^{13}$C-labelled $CO_2$ was traced in two *c*. 90-year-old *P. sylvestris* trees

153    growing at the Rosinedalsheden experimental forest in northern Sweden (64°10′N, 19°45′E,

154    153 m above sea level) in the late-summer of 2014. At the time of the experiment, the studied

155    trees had diameters at 1.3 m of 18.0 cm (Tree 1) and 20.6 cm (Tree 2), corresponding to 49th

156    and 72nd percentile on the stand-scale (Tarvainen et al. 2018), and were 15.8 and 16.4 m tall,

157    respectively. Tree 1 was located northeast and Tree 2 southeast of the scaffolding tower used

158    to access the upper boles and the shoots. The mean temperature and relative humidity, and

159    the total precipitation during the experiment were 11.3 °C, 86.6% and 33 mm, respectively.

160    The site is described in more detail in: Lim et al. (2015), stand structure; Hasselquist et al.

161    (2012), soil properties; and Tarvainen et al. (2016) and Tarvainen et al. (2018), foliar and

162    stem properties, respectively.

163

164    *Labelling*

165    *Label preparation and infusion*

166    The $^{13}$C label was introduced to the stems as 5 g of 99% $^{13}$C Na$^+$H$^{13}$CO$^{-3}$ solution dissolved

167    in 100 ml de-ionized water (solution pH = 8.3) at the height of 0.6 m above ground on the

168    northwestern side of Tree 1 and southeastern side of the Tree 2 on the 22nd of August 2014.

169    The label was infused into a 5.5 cm deep hole with a diameter of 6 mm. The holes were

170    rinsed for 30 seconds with acetone immediately after drilling and again before the labelling

171    the next day. The acetone dissolved resin and presumably killed some of the resin

172    parenchyma cells on the walls of the hole. The residual acetone then evaporated or was

173    dissolved into the xylem sap and disappeared. This method has been extensively used in

174    *Pinus sylvestris* in previous studies. We inserted tapered tip of a 6 mm diameter tube into the

175  hole. The tube was not sealed except by the tight fit of the tube insertion. The tube was

176  attached to a standard polypropylene squeeze bottle of the type commonly used for laboratory

177  solvents. The label solution was poured inside the squeeze bottle, which was then mounted

178  upside-down on the tree stem and left for three days, at which time it had been taken up by

179  the tree.

180

181  *Label spread and transport inside the stem*

182  When the label was injected into the xylem, we envision that it created a cylindrical bolus

183  around the hole drilled into the sapwood. The pH at the center of the bolus would have been

184  8.3 and the osmotic potential would have been *c*. -3 MPa, as determined by the original

185  composition of 5 g of $Na^+H^{13}CO^{-3}$/100 mL de-ionized water. The initial $CO_2$ concentration of

186  the solution would have been approximately 8000 $\mu mol\ mol^{-1}$, as defined by the Henry's Law

187  constants (Teskey et al. 2008). In pines, injected dyes spread in a fan-shaped pattern that

188  encircles the tree within a meter or so of the injection point (Vite and Rudinsky 1959). We

189  presumed this label would do the same.

190          As the pH of labelled water fell, bicarbonate would be converted to carbonic

191  acid and thence to $CO_2$. The dissolved $CO_2$ would then outgas from the xylem stream into the

192  air spaces in the cell walls (Gartner et al. 2004, Sorz and Hietz, 2006). Via these air spaces, it

193  would diffuse to the bark, conducted by the much higher diffusivity in the gas phase than in

194  liquid water and driven by the steep $CO_2$ concentration gradient from the tree center to the

195  bark surface. At the same time, the dissolved inorganic carbon would move upward with the

196  xylem water flux. The central question of this manuscript is about the comparison between

197  the radial diffusion rate and the upward dissolved flux.

198

199  **Measurements**

*Measurement timeline*

200

201  The vertical patterns of stem $CO_2$ efflux and its isotopic enrichment, the refixation of the

202  outward diffusing $CO_2$ by corticular photosynthesis, and top of the canopy shoot-scale gas

203  exchange were monitored continuously from the 22nd of August until the 13th of September,

204  using the same experimental set up as in Tarvainen et al. (2018). Samples for determination

205  of xylem sap composition and pH, and tissue ^{13}C enrichment were collected intermittently

206  from the start of the experiment until the 7th of October. The timing of the various

207  measurements is presented in the supplementary table S1.

208

*Gas exchange and online ^{13}C enrichment measurements*

209

210  The $CO_2$ efflux from the stem was observed continuously utilising a custom-built automatic

211  gas-exchange system (Wallin et al. 2001, Tarvainen et al. 2018) working in open

212  configuration.  The chambers for the stem measurements were made out of transparent

213  acrylic plastic (Perspex) and covered a surface area varying between 109 and 126 cm$^2$

214  depending on the shape of the bole at the chamber location. Adjustable straps were used to

215  mount the chambers at four heights along the bole; low bole (1.5 m), below crown (5.3 m),

216  low crown (9.2 m), and mid-crown (Tree 1 11.6 m; Tree 2 12.5 m). We deliberately chose a

217  design that emphasised the measurement of the vertical patterns of gas exchange and isotopic

218  composition over replication of single height measurements on a greater number of individual

219  trees (within the technical limits on the number of measurement chambers). This choice was

220  made because the main aim of the tracer experiment was to follow the ^{13}C label along the

221  bole to get a comprehensive picture of the label distribution rather than a snapshot of the label

222  efflux at a given point of the stem. The chambers covered only a portion of the circumference

223  of the bole, but the small size had the benefit of allowing chambers to be placed within the

224  crown despite dense branching. The positioning and radial coverage of the stem chambers is

225 summarized in the supplementary table S2. To enhance turbulence and mixing within the

226 chambers the incoming ambient air was led through a bent piece of tubing directing the flow

227 toward the chamber wall.

228 The gas exchange and the $^{13}C$ label efflux were also observed on one one-year-old

229 upper canopy shoot on each studied tree using the same custom-built system. For these

230 measurements, 55 mm long shoot segments were inserted into transparent shoot chambers

231 controlled to track ambient temperature and equipped with fans to ensure the mixing of the

232 air (Wallin et al. 2001, Tarvainen et al. 2016). The chamber temperatures differed from the

233 ambient by $-0.01 \pm 0.18$ °C (mean ± SD, $n = 1085$) and $0.01 \pm 0.40$ °C ($n = 1088$) for Tree 1

234 and Tree 2, respectively, between the 22nd of August and the 13th of September. The

235 photosynthetic photon flux density at the shoot positions and the relative humidity inside the

236 shoot chambers are shown in supplementary figure S1. Diaphragm pumps were used to draw

237 the sample air from the stem and shoot chambers through insulated and heated tubing at the

238 rate of $0.5$ l min$^{-1}$ to a nearby hut that housed the instrumentation. The $CO_2$ concentrations in

239 the sample air were measured using an infrared gas analyser (CIRAS-1, PP Systems, Hitchin

240 Herts, UK), and compared to simultaneous measurements of adjacent empty reference

241 chambers. The exhaust vent of the gas exchange system was connected to a Picarro G2131-$i$

242 isotopic analyser (Picarro Inc. Santa Clara, CA, U.S.A.) allowing for simultaneous

243 measurements of the $^{13}C$ enrichment of the sample airflow. Each sample position was

244 measured for 300 seconds by both instruments following a flow stabilisation period of 540

245 seconds. The system is divided into two parts, each with its own pump, controlling the flow

246 from up to six measurement positions. Each chamber is continuously ventilated. This allows

247 for sample airflow from one part of the system to stabilize during the measurement of the

248 airflow from the other part, reducing the overall waiting time between subsequent

249    measurements. In this experiment, the sample rate was once every 74 minutes per chamber

250    position. Additional details on the setup can be found in Tarvainen et al. (2018).

251

252    *Xylem sap $CO_2$ concentration and $^{13}C$ enrichment*

253    Xylem sap was sampled by equilibrium tubes as described in Ubierna et al. (2009) and

254    Powers and Marshall (2011) at all heights with stem chambers on each studied tree on the

255    27th of August and, 1st and 4th of September. The equilibrium tubes were inserted *c*. 50 cm

256    above the stem chambers. Briefly, a stainless steel tube was inserted into the perpendicular

257    end of a T-fitting. A rubber septum was inserted in the cap of the top end of the T-fitting and

258    the bottom end was connected to a non-permeable tubing capped with a rubber septum in the

259    end away from the T-fitting. The stainless steel tube was hammered into a 3 cm deep hole

260    drilled into the stem. No further sealing was necessary. The gas contained in the bole could

261    thus diffuse into and equilibrate with the headspace of the non-permeable tubing. To sample

262    the stem gas, an empty syringe was inserted in the top septum and the equilibrated headspace

263    gas forced into it by pushing acidified water into the non-permeable tubing through the

264    bottom septum. Note that if there had been a leak, this operation would have failed because

265    the pressurised gas would have flown into the surrounding atmosphere rather than the empty

266    syringe. Finally, the gas collected in the upper syringe was inserted into 12 ml evacuated

267    glass vials with exetainer caps. The samples were analysed by a Thermo Isotope Ratio Mass

268    Spectrometer (IRMS, DeltaV plus with GasBench II). Only the samples collected from the

269    1.5 m and 5.3 m vertical positions were used in the analyses presented here because resin

270    production blocked access to the headspace in the upper stem positions.

271

272    *Tissue $^{13}C$ enrichment*

1
2
3
4
5
6
7
8
9
10
11
12
13
14
15
16
17
18
19
20
21
22
23
24
25
26
27
28
29
30
31
32
33
34
35
36
37
38
39
40
41
42
43
44
45
46
47
48
49
50
51
52
53
54
55
56
57
58
59
60

273  Samples were collected from all positions included in the gas exchange measurements to

274  determine if $^{13}C$ was being incorporated in the phloem and needle tissues. Sampling was

275  conducted once during the gas exchange measurements (27th of August, five days after the

276  label infusion) and twice afterwards (17th and 22nd of September). Only phloem samples were

277  collected on September 22nd. The needle samples were collected from branches close to those

278  measured by the gas exchange system. The phloem samples were collected with a 10 mm

279  diameter punch within 25 cm of each bole chamber on the side of the tree with the chamber

280  except for Tree 2 at 1.5 m, where it was done on the opposite side of the chamber. The

281  phloem sample locations are summarized in supplementary Table S2. The isotopic

282  composition of the tissue C in the samples was determined after combustion using the

283  Elemental Analyser - Isotope Ratio Mass Spectrometer (EA-IRMS) technique (Werner et al.

284  1999). A Flash EA 2000 (Thermo Fisher Scientific, Bremen, Germany) elemental analyser

285  and a DeltaV (Thermo Fisher Scientific, Bremen, Germany) spectrometer were used for these

286  analyses. We note that the samples were not acidified prior to analysis and the results thus,

287  reflect the isotopic composition of any inorganic C in the water associated with the sampled

288  phloem and needle tissues.

289

290  *Xylem sap pH*

291  The pH of the xylem sap was determined from one mid-crown branch from each of the two

292  trees included in the study and six additional adjacent trees. The branches were cut using a

293  saw, on the 7th of October and transported to the laboratory where they were then stored at 4

294  °C in darkness until the pH measurements were made on the 15th to 17th of October. The

295  indoor temperature during the pH measurement was c. 23 °C. The sample branches were

296  recut under water and the bark removed with a knife prior to the xylem sap extraction. The

297  length of the branch sections chosen for analysis was 20 - 30 cm. The sap was extracted using

298   the water displacement method (e.g. Glavac et al. 1990). This method cuts living parenchyma

299   cells at the ends of the branch section, spilling cell contents into the collected sap, but only at

300   the beginning of the extraction. As the extraction proceeds, pure xylem water is expressed

301   without further contamination by cell contents. Specifically, a branch was first fastened to

302   one end of a 25 mm diameter PVC tube, then *c*. 600 ml deionized water including food

303   colouring (Dr. Oetker Sverige AB, Gothenburg, Sweden; blue, pH 3.37) was poured into the

304   tube. The resulting pressure pushed out the xylem sap, which was collected in 1.5 ml

305   Eppendorf vials until the arrival of coloured water. The pH of each sample vial was measured

306   immediately following the sap extraction using a PHM202 pH meter (Radiometer,

307   Copenhagen, Denmark). The last pH measurement made before the arrival of the coloured

308   water was used in the mass balance calculations described below. The pH meter was

309   calibrated using known buffers (pH 4.00 and pH 7.00) and the sensor head rinsed with

310   deionized water between measurements on different branches.

311

312   *Sap flow, stem temperature and environmental variables*

313   Sap flow measurements were made half-hourly at breast height using Granier-type sensors

314   (Tor-Ngren et al. 2017). A previously developed relationship between vapour pressure

315   deficit, photosynthetic photon flux density (PPFD), and sap flow (Tor-Ngren et al. 2017) was

316   used for gap-filling when data were missing due to instrument malfunction (60% of the data).

317   The stem temperature ($T_s$) was measured continuously by copper-constantan thermocouples

318   inserted at 5 mm and 40 mm depths in the stem at each measurement position. The

319   environmental data were collected at a nearby sub-site (< 2 km away) within the same

320   experimental Scots pine stand. A HC2-S3 probe (Rotronic AG, Bassersdorf, Switzerland)

321   installed in a ventilated radiation shield (In Situ, Ockelbo, Sweden) was used to record half-

1
2
3
4
5
6
7
8
9
10
11
12
13
14
15
16
17
18
19
20
21
22
23
24
25
26
27
28
29
30
31
32
33
34
35
36
37
38
39
40
41
42
43
44
45
46
47
48
49
50
51
52
53
54
55
56
57
58
59
60

322    hourly mean air temperature and humidity (1.5 m aboveground). A Li-190SA PPFD-sensor

323    (Licor Biosciences, Lincoln, NE, USA) was used to measure above-canopy PPFD.

324

325    ***Data analysis***

326    *Mass balance calculation*

327    Henry's law was used to calculate half-hourly values of the amount of $CO_2$ dissolved in the

328    xylem sap ([$CO_2$*]) from the observed pH, $CO_2$ partial pressure ($pCO_2$) at the given date, and

329    the continuously measured $T_s$ at 40 mm depth in the stem segment spanning from 1.5 m to

330    5.3 m in each tree (eq. 1):

331

332    $$[CO_2^*] = \left(1 + \frac{K_1}{10^{-pH}} + \frac{K_1 K_2}{(10^{-pH})^2}\right) K_H pCO_2 \qquad \text{(eq. 1)}$$

333

334    where $K_1$, $K_2$ and $K_H$ are the solubility constants that depend on $T_s$. These constants were

335    calculated according to McGuire and Teskey (2002):

336

337    $$K_1 = (2.5764 \times 10^{-7}) + (3.3742 \times 10^{-7})(1 - e^{-0.0318T_s}) \qquad \text{(eq. 2)}$$

338

339    $$K_2 = (2.3777 \times 10^{-11}) + (9.0041 \times 10^{-13})T_s \qquad \text{(eq. 3)}$$

340

341    $$K_H = 0.0114 + 0.0661e^{-0.0433T_s} \qquad \text{(eq. 4)}$$

342

343    The transport rate of $CO_2$ in the xylem was then determined by multiplying the difference in

344    [$CO_2$*] between the two measurement positions by the half-hourly observations of sap flow

345    rate (McGuire and Teskey 2004). The total $CO_2$ budget of the bole volume was assessed

346    using the mass balance approach (eq. 5, McGuire and Teskey 2004) modified to include

347    cortical $CO_2$ assimilation. According to this approach the total respiration from a stem

348    segment ($R_S$) can be expressed as,

349

350    $$R_S = E_C + A_R + F_T + \Delta S \qquad\qquad\qquad\qquad\qquad \text{(eq. 5)}$$

351

352    where $E_c$ is $CO_2$ efflux to atmosphere measured using transparent chambers allowing for $A_R$,

353    which is the rate of local cortical $CO_2$ assimilation (*i.e.* refixation), $F_T$ is the net sap $CO_2$

354    transport flux (i.e. transport efflux – transport influx) and $\Delta S$ the storage flux (change in mean

355    xylem [$CO_2$] over time). The net $E_c$ was measured continuously at 1.5 m and 5.3 m by the

356    chamber system and upscaled to the entire bole segment assuming linear change in $E_c$

357    between the measurement heights as in Tarvainen et al. (2018). The magnitude of $A_R$ was

358    estimated as the difference between the observed $E_c$ and $E_c$ in absence of refixation ($E_{dark}$).

359    $E_{dark}$ was predicted based on the relationship between $E_c$ and $T_s$ at 5 mm depth at night when

360    no cortical $CO_2$ assimilation occurs. First, an exponential function was fitted to night-time

361    (above-canopy PPFD < 2 $\mu$mol m$^{-2}$ s$^{-1}$) measurements of $E_c$ and $T_s$ to obtain coefficients

362    representing base dark respiration rate and the temperature response of the dark respiration.

363    These coefficients were then used to predict daytime $E_{dark}$ based on the continuously

364    measured $T_s$ data (5 mm depth, see Tarvainen et al. 2018 for additional details of the fitting

365    procedure). In order to obtain a sufficiently large temperature range for reliable curve fitting,

366    the sensitivity of night-time $E_c$ to $T_s$ was determined from observations made between the

367    25th of August and 6th of September, thus spanning a period from two days prior to first

368    sampling of the equilibrium tubes until two days after the last sampling. Similarly to $E_c$, when

369    calculating $A_R$ of the entire bole segment the rate of cortical refixation of $CO_2$ was assumed

370    to increase linearly between the two heights. As shown in Tarvainen et al. (2018) $A_R$ was zero

371    at 1.5 m where no chlorophyll was present in the stem tissues, while at 5.3 m where the bark

372    tissue contained chlorophyll the daily mean $A_R$ corresponded to *c*. 16% of the predicted $E_{dark}$.

373    The temperature response fits for the three days for which mass balance was calculated are

374    given in Table S3.

375        We note that predicting daytime stem $CO_2$ efflux from night-time data requires

376    assuming that diurnally variable processes potentially affecting the response, such as changes

377    in cell turgor (Saveyn et al. 2007, Salomón et al. 2018) or $CO_2$ transport in the xylem, are

378    negligible. Based on the diurnal pattern of hysteresis between stem $E_c$ and $T_s$ it has been

379    suggested that xylem $CO_2$ transport is of limited importance the trees included in the current

380    study (Tarvainen et al., 2018). This finding will be more rigorously tested in the current

381    study. As the mass balance calculations utilised data collected over single days change in

382    $CO_2$ storage within the stem volume was assumed negligible. This assumption is supported

383    by previous studies that have estimated the storage change over 24 h to < 3% in *Platanus*

384    *occidentalis* L. (sycamore), *Liquidambar styraciflua* L. (sweetgum) and *Dacrydium*

385    *cupressinum* L. (rimu) (McGuire and Teskey 2004, Bowman et al. 2005, Teskey and

386    McGuire 2007). We note, however, that a higher change, 8%, has been reported for *Fagus*

387    *grandifolia* Ehrh. (American beech) (McGuire and Teskey 2004).

388        To facilitate comparisons with previous studies the mass balance fluxes are presented

389    per unit sapwood volume of the studied bole segment. The total bole segment volume,

390    including bark and heartwood, was calculated assuming that it was shaped as a conical

391    frustum. This volume was multiplied by 0.84 to account for bark volume, based on previous

392    work at the current site (Lim et al. 2015), thus yielding total wood volume. The total wood

393    volume was then multiplied by 0.71, the sapwood fraction observed from stem discs collected

394    at the site (Ruth Magh, personal communication), for the final sapwood volume estimate.

395    When estimating the rate of sap rise based on the sap flow measurements the volume was

396    further multiplied by 0.68 to account for porosity (Usta 2003).

397

398    **Results**

399    *Stem temperatures and sap flow*

400    The variations in $T_s$ at 40 mm depth, sap flow rate and PPFD the week before the experiment

401    and during the three-week period during which the ^{13}C label efflux was continuously

402    monitored are shown in Figure 1. The mean daily $T_s$ varied little over the experiment. Sap

403    flow was more variable with peaks during clear days and the lowest values on cloudy days

404    with low PPFD, the latter coinciding with low diurnal $T_s$ amplitudes during the early part of

405    the experiment (Figure 1).

406

407    *[13]C enrichment*

408    The ^{13}C enrichment observed in the chamber efflux decreased strongly with height above

409    ground (Figure 2, note the differences on y-axis scales among the measurement positions),

410    suggesting limited upward transport of $CO_2$ in the xylem of the studied trees. We note that

411    very little ^{13}C reached the breast height chamber of Tree 2 (Figure 2e). This was likely

412    because the chamber was placed on the opposite side of the bole from the label infusion

413    point. We suspect that the distance (0.9 m) between these two positions was too short to

414    allow for sufficient radial dispersal of the label for a strong ^{13}C signal to be observable in the

415    breast height chamber. This assumption is supported by the strong ^{13}C enrichment observed

416    in the xylem sap (Figure 3) and phloem tissue (Figure 4) samples from this position during

417    the first sampling that was conducted five days after the start of the labelling. However, the

418    overall pattern of vertically decreasing label recovery is clear when comparing the other

1
2
3
4
5
6
7
8
9
10
11
12
13
14
15
16
17
18
19
20
21
22
23
24
25
26
27
28
29
30
31
32
33
34
35
36
37
38
39
40
41
42
43
44
45
46
47
48
49
50
51
52
53
54
55
56
57
58
59
60

419  chambers on this tree. Furthermore, the greater tissue $^{13}C$ enrichment observed at 5.3 m on

420  the 17th of September than at 1.5 m on the 27th of August (Figure 4) suggests that while the

421  label was present in the xylem sap (Figure 3) and in the $CO_2$ efflux (Figure 2) at 1.5 m on

422  August 27th it was not incorporated in the phloem tissues. Overall, the tissue $^{13}C$ analyses

423  showed that the phloem became enriched at 1.5 m, albeit weakly, and at 5.3 m during the

424  experiment while no evidence of enrichment was seen in the upper bole or the needle samples

425  (Figure 4).The continuous observations of $^{13}C$ recovery during much of the 25th of August

426  were lost to an inopportune computer failure.

427       Despite the differences in absolute $^{13}C$ recovery between the trees, the timing of the

428  maximum mean daily enrichment observed at the various measurement heights suggests that

429  the xylem $CO_2$ transport rate was similar, 0.95 m d$^{-1}$, between the two trees (slope in Figure

430  5). Although more infrequent, the xylem sap samples collected by the equilibrium tubes

431  yielded similar estimates of the time to peak $^{13}C$ enrichment (Figure 3) at 1.5 and 5.3 m as the

432  continuous isotope data (Figure 5). Rate of sap rise calculated from sap flow data and tree

433  dimensions was similar to the isotopic estimate, 1.09 m d$^{-1}$.

434

435  *Mass balance*

436  Sap pH was 6.1 in both of the studied trees, and comparable to the mean of all of the sampled

437  trees at the site, $6.2 \pm 0.1$ (mean $\pm$ SD, $n = 8$). The [$CO_2$] of the xylem sap on three dates

438  during the study period are shown in Table 1. The mass balance calculation indicated that a

439  vast majority of the local respiration diffused radially out of the stem in both sample trees

440  and, thus, was the main driver of the observed net $CO_2$ efflux ($E_c$). Corticular refixation ($A_R$)

441  was the second most important determinant of the $CO_2$ budget. The relative magnitude of

442  xylem transport ($F_T$) compared to the total respiration ($R_s$) of the bole segment was less than

443  6% (Table 2).

444

445

**Discussion**

The minute amount of the $^{13}$C tracer detected above breast height in the continuous

measurements of stem effluxes strongly suggests that little labelled C was transported up the

stem in the xylem of the studied mature *P. sylvestris* trees (hypothesis #1) and that it instead

rapidly diffused out from the lower stem. This finding was supported by the mass balance

calculations that indicated that most of the $CO_2$ efflux from the bole originated from local

respiration (hypothesis #2), and further by the tissue sample analyses finding no evidence of

$^{13}$C enrichment in the phloem contents of the upper bole or in the needles. Taken together our

results support the notion that chamber-based measurements of soil and stem $CO_2$ efflux, and

foliar photosynthesis are not much biased by $CO_2$ transport along the root-stem-leaf

continuum in large *P. sylvestris* trees. This agrees with previous findings on other conifers

(e.g. Ford et al. 2007, Ubierna et al. 2009, Powers and Marshall 2011, but see Zelawski et al.

1970), but contrasts the results from studies on ring- and diffuse-porous species (e.g. Teskey

and McGuire 2002, McGuire et al. 2007, Saveyn et al. 2008, Bloemen et al. 2013a, Salomón

et al. 2019)

Several trait differences, including sap flow rates, xylem [$CO_2$] and pH, and tree growth

rates, may contribute to such among-species differences in the importance of xylem $CO_2$

transport. Furthermore, each of these factors exhibits seasonal and/or diel variation

suggesting that the timing of a given study may influence its conclusions. Sap flow rates are

commonly higher in species with significant xylem $CO_2$ transport compared to species with

limited xylem transport reflecting their different wood anatomies (Ubierna et al. 2009). The

current experiment, carried out from mid-August to mid-September, coincided with the

period when tree-scale transpiration rate begins to decline in response to decreasing light

1
2
3
4
5
6
7
8
9
10
11
12
13
14
15
16
17
18
19
20
21
22
23
24
25
26
27
28
29
30
31
32
33
34
35
36
37
38
39
40
41
42
43
44
45
46
47
48
49
50
51
52
53
54
55
56
57
58
59
60

469    availability and vapour pressure deficit (Tor-ngern et al. 2017). However, with other things

470    being equal, a 50% increase in the sap flow rate, and thus a 50% increase in $F_T$, would still

471    have led to relatively low $F_T$ to $R_s$ ratios (Table 2).

472       Xylem [$CO_2$] has been reported to vary from close to 0% to 26.3% (Teskey et al. 2008

473    and references therein). Our observed [$CO_2$], ~ 0.27% to ~ 0.99%, is thus at the lower end of

474    the reported range. Because the calculation of $F_T$ through a stem segment is based on the

475    difference in [$CO_2$] between the upper and lower ends of the segment, a similar relative [$CO_2$]

476    difference would yield higher estimates of $F_T$ if the absolute [$CO_2$] differences were greater,

477    and subsequently increase $F_T/R_s$. Thus, low xylem [$CO_2$] in conifers could explain the

478    among-species differences in observed $CO_2$ transport. However, although ring- and diffuse-

479    porous angiosperms account for the highest xylem [$CO_2$] observations, it is not readily

480    apparent from reported data that conifers would have generally lower xylem [$CO_2$] than

481    angiosperms (see Table 1 in Teskey et al. 2008). In addition to among-species variation,

482    xylem [$CO_2$] has also been shown to vary seasonally and diurnally (e.g. Etzold et al. 2013,

483    Erda et al. 2014, Salomón et al. 2016). Such patterns have been related to variation in

484    temperature and are, over the seasonal scale, also influenced by the timing of growth (Etzold

485    et al. 2013). Furthermore, seasonal and diel changes in water availability and humidity

486    influence the radial diffusion velocity of $CO_2$ (Sorz and Hietz 2006, Steppe et al. 2007), and

487    naturally also sap flow rates. Accordingly, increased xylem [$CO_2$] has been observed after

488    rain events and attributed in part to reduced radial diffusion (Salomón et al. 2016).

489       There was considerable variation in the xylem sap [$CO_2$] determined from samples

490    collected using equilibrium tubes among the trees, measurement heights and dates (Table 1).

491    Several factors may have contributed to such variation. Potential mechanistic causes include

492    differences in: i) the stem temperatures, ii) the depths at which the equilibrium tubes were

493    inserted, iii) the rates of corticular refixation of $CO_2$ (Tarvainen et al. 2018), and iv) the rates

494    of stem growth during the studied late summer period. Furthermore, the infusion of the

495    bicarbonate solution used in the labelling and its movement within the xylem, as well as a

496    time lag between changes occurring inside the xylem and observable changes in the

497    equilibrium tubes may have affected the veracity of the xylem $[CO_2]$ observations. Also, $CO_2$

498    use in local biosynthesis reactions involving PEPC (Berveiller and Damesin 2008, Hilman et

499    al. 2019) could bias mass balance derived estimates of xylem $CO_2$ transport rates. We further

500    note that we determined $A_R$ in the modified mass balance equation by a comparison of night-

501    and daytime stem efflux data. This comparison could be biased by diurnal variation in cell

502    turgor pressure (Saveyn et al. 2007, Salomón et al. 2018) or in xylem $CO_2$ transport. We did

503    not evaluate the former but note that we previously found no diurnal hysteresis between $E_c$

504    and $T_s$ in the lower stems where refixation was hindered by the thick bark and lack of light

505    (Tarvainen et al. 2018), suggesting the absence of significant turgor pressure or xylem

506    transport related changes in $E_c$ at this site. In addition, the findings of this study suggest that

507    xylem $CO_2$ transport was of limited importance for the stem $CO_2$ budget. Despite such

508    potential confounding factors, the mass balance calculations and the isotopic method led to

509    similar conclusions regarding the sources and the fate of xylem $CO_2$ in the current study. The

510    uncertainties associated with the determination of the xylem sap $[CO_2]$ and role of within-

511    stem $CO_2$ cycling, however, highlight the usefulness of isotope ratios for assessing $CO_2$

512    dynamics in tree stems as labelling causes the isotope ratios to rise into a range that would

513    otherwise never occur thereby removing any ambiguity regarding the observations.

514        Naturally, there are also uncertainties associated with methods that use isotopes to infer

515    stem $CO_2$ budgets as was done here. As the outgassing $^{13}CO_2$ passed through the bark, some

516    portion would be refixed by the chlorophyllous tissues in the periderm (Pfanz et al. 2002,

517    Wittmann et al. 2006, Tarvainen et al. 2018) as noted in our formulation of the mass balance

518    equation. The refixed $^{13}CO_2$ would presumably be loaded into the phloem, where it would

519    show up in the phloem samples (Figure 4). Notably, the refixation, and thus label

520    incorporation in the phloem tissue, was greater at 5.3 m (c. 16 % refixation) than at 1.5 m (<

521    2.5 % refixation) (Tarvainen et al. 2018 and Figure 4, respectively). That phloem label would

522    be entrained in the downward transport in the phloem (Powers & Marshall, 2011). The

523    remainder of the outgassing label diffused out into the atmosphere and was therefore detected

524    by the Picarro analyser connected to the stem chambers. Any missing $CO_2$ was presumably

525    carried in solution upwards in the xylem stream. Note that if the xylem stream contained

526    dissolved $^{13}CO_2$, it would show up in the equilibration tubes, which provided a headspace in

527    contact with the xylem water in the stem (Figure 3).

528        Based on the extensive literature about vertical $CO_2$ transport (e.g. McGuire and

529    Teskey 2004, Teskey et al. 2008, Bloemen et al. 2013a, Salomón et al. 2019), one might

530    expect that the bolus of saturated bicarbonate solution would carry the label far up the tree.

531    This is particularly true because the water would move under piston flow (Marshall et al.,

532    2020), with relatively little mixing into the surrounding xylem water; the water contents of

533    the tracheids would be replaced by root water being pulled up from below. One might worry

534    that the low buffering capacity of xylem water would be slow to titrate the alkalinity in the

535    bolus, allowing the label to continue up the stem as highly soluble bicarbonate, but this would

536    overestimate the upward flux and underestimate radial diffusion. Alternatively, one might

537    worry about a release of labeled $CO_2$ so rapid that it would leave the stem before it had had a

538    chance to dissolve into the xylem. However, we saw a strong label signal in the $CO_2$ efflux

539    approximately 1 m above the injection point. For this to be the case, the label must have

540    moved upward through or around the xylem contents. It would be surprising if the label could

541    move diagonally upward and radially outward without at least partially dissolving into the

542    water in the tracheids. It therefore seems likely that the label had the opportunity to dissolve

543    into the xylem water and be carried up the stem; it is only that the alternative, the radial

544  diffusion path out of the stem, was so much faster. Of course, this relates directly to the

545  relatively minor role of vertical dissolution transport in these pine trees.

546      The [$CO_2$*] increases rapidly when pH increases above ~ 6 (e.g. Levy et al. 1999, Erda

547  et al. 2014) in response to increasing solubility of the $HCO_3^-$ species of the carbonate

548  equilibrium system. Reports on xylem pH in trees span from < 4 to > 7 (Teskey et al. 2008).

549  Therefore, systematic variation in sap pH could explain the among-species differences in

550  xylem transport of $CO_2$ and its equilibrium species. However, few studies have compared the

551  sap pH of different species exposed to the same environmental conditions. Thomas and

552  Eamus (2002) measured the xylem pH of six savanna tree species; two each of evergreen,

553  semi-deciduous, and deciduous. The observed pH ranges were similar for all of the studied

554  species. A study on 22 perennials grown under controlled conditions in pots found among

555  species differences in xylem pH that exceeded three pH units under well-watered conditions

556  (Sharp and Davies 2009). In addition, like [$CO_2$], sap pH exhibits seasonal and diel variation

557  of up to 0.5 pH units (e.g. Erda et al. 2014, Salomón et al. 2016). Thus, the timing of the sap

558  sampling may also affect the estimates of xylem $CO_2$ transport capacity. The pH observed

559  here is similar to data from other *P. sylvestris* stands (Perks et al. 2002, Tarvainen

560  unpublished data). We note that, with all other things being equal, 0.5 unit lower pH would

561  have reduced $F_T$ by 20 - 25%, while 0.5 unit higher pH would have increased $F_T$ by 65 - 70%

562  in Table 2. Given the low [$CO_2$*] of the studied trees this would, however, have yielded

563  relatively minor changes for the importance of $F_T$ (mean $F_T$-to-$R_S$ % for -0.5 pH, observed

564  pH and +0.5 pH: 2.1%, 2.6% and 4.4%, respectively).

565      Collectively, the expected seasonal variations in sap flow, xylem [$CO_2$] and pH make it

566  likely that more $CO_2$ is transported by the xylem of the studied *P. sylvestris* trees during the

567  months when stem and root growth are the strongest. This would agree with the findings of

568  Etzold et al. (2013) who studied sap flow and xylem [$CO_2$] in *Picea abies* L. Karst. (Norway

569  spruce) trees and suggested that xylem $CO_2$ transport may be seasonally variable, peaking

570  during most active root growth. However, local respiration will also be greater during the

571  main growing period in response to both the growth itself and the high summertime

572  temperatures increasing growth and maintenance respiration (Stockfors and Linder 1998),

573  respectively. Furthermore, it has been shown that stem $CO_2$ efflux rates may vary along the

574  bole in response to vertical growth patterns (e.g. Araki et al. 2010, Tarvainen et al. 2014)

575  suggesting that mass balance-based estimates relying on measurements made only in the

576  lower bole may not be representative of the entire tree during the growing season. Thus,

577  confidently assessing the net effect of seasonality in xylem $CO_2$ transport on stem $CO_2$ fluxes

578  would require long-term measurements made at several positions along the bole and the

579  branches.

580      Overall, we agree with Salomón et al. (2019) in that the isotopic approach has great

581  potential for informing about $CO_2$ movement in stems, including in mature field-grown trees

582  as reported here. Future studies will benefit from using chambers that enclose the entire stem

583  circumference to ensure that label is not missed in cases where the vertical spread is slow, as

584  also recommended by Salomón et al. (2019) based on their glasshouse study. The spatial and

585  temporal flux patterns presented here may guide experimental design regarding along stems

586  and among-trees replication as well as the choice of the type and vertical positioning of the

587  chambers to improve the robustness of the findings of future studies. Furthermore, we note

588  that when measuring the $CO_2$ budgets of conifers it will important to pay close attention to

589  resin production to avoid loss of xylem water $[CO_2]$ or $^{13}C$ enrichment data.

590      In summary, we combined, for the first time, isotopic labeling and CRDS technology to

591  study stem carbon cycling in field-grown trees. We used this methodology and two other

592  independent methods, mass balance calculations and tissue sampling, to evaluate xylem

593  transport of dissolved $CO_2$ in mature *P. sylvestris* trees. All the methods indicated that little

594     $CO_2$ was transported up the bole during the studied late summer period. Furthermore, mass

595     balance calculations showed that most of the local respiration diffused radially to the

596     atmosphere and was included in the observed stem $CO_2$ efflux. Based on these results, and

597     the previous work on conifers yielding similar findings, we conclude that the concerns

598     regarding the suitability of chamber-based methods for estimating the partitioning of root and

599     stem respiration, due to sap-mediated vertical movement of $CO_2$, may be unwarranted for

600     mature conifer stands. It is, however, still unclear what causes the observed differences in the

601     importance of xylem $CO_2$ transport between species with tracheid and ring- or diffuse-porous

602     anatomies. Therefore, we suggest that future work on xylem $CO_2$ transport should include

603     experiments where species with different wood anatomy are studied with the same methods

604     under the same environmental conditions.

605

**Supplementary Data**

607     Supplementary Data for this article are available at *Tree Physiology* Online.

608

**Conflict of Interest**

610     None declared.

611

**Funding**

**Acknowledgements**

**Authors' Contributions**

633    L.T., G.W., M.R. and J.D.M. designed the experiment and performed the gas exchange and

634    isotopic measurements and sample collection. M.O.L. collected the environmental data. R.O.

635    and P.T. collected and analysed the sapflux data. L.T. and J.D.M. analysed the gas exchange

636    and isotopic data, and wrote the manuscript. All authors provided editorial advice and

637    approved the final manuscript.

638

639    **References**

640    Angert A, Muhr J, Negron Juarez R, Alegria Muñoz W, Kraemer G, Ramirez Santillan J,

641        Barkan E, Mazeh S, Chambers JG, Trumbore SE (2012) Internal respiration of Amazon

642        tree stems greatly exceeds external $CO_2$ efflux. Biogeosciences 9:4979-4991.

643    Araki MG, Utsugi H, Kajimoto T, Han Q, Kawasaki T, Chiba Y (2010) Estimation of whole-

644        stem respiration, incorporating vertical and seasonal variations in stem $CO_2$ efflux rate, of

645        *Chamaecyparis obtusa* trees. J For Res 15:115-122.

646    Aubrey DP, Teskey RO (2009) Root-derived $CO_2$ efflux via xylem stream rivals soil $CO_2$

647        efflux. New Phytol 184:35-40.

648    Berveiller D, Damesin C (2008) Carbon assimilation by tree stems: potential involvement of

649        phosphoenolpyruvate carboxylase. Trees 22:149-157.

650    Bloemen J, McGuire MA, Aubrey DP, Teskey RO, Steppe K (2013a) Transport of root-

651        respired $CO_2$ via the transpiration stream affects aboveground carbon assimilation and

652        $CO_2$ efflux in trees. New Phytol 197:555-565.

653    Bloemen J, McGuire MA, Aubrey DP, Teskey RO, Steppe K (2013b). Assimilation of

654        xylem-transported $CO_2$ is dependent on transpiration rate but is small relative to

655        atmospheric fixation. J Exp Bot 64:2129-2138.

656    Bowman WP, Barbour MM, Turnbull MH, Tissue DT, Whitehead D, Griffin KL (2005) Sap

657        flow rates and sapwood density are critical factors in within- and between-tree variation in

658        $CO_2$ efflux from stems of mature *Dacrydium cupressinum* trees. New Phytol 167:815-828.

659    Erda FG, Bloemen J, Steppe K (2014) Quantifying the impact of daily and seasonal variation

660        in sap pH on xylem dissolved inorganic carbon estimates in plum trees. Plant Biol 16:43-

661        48.

662  Etzold S, Zweifel R, Ruehr NK, Eugster W, Buchmann N (2013) Long-term stem $CO_2$

663      concentration measurements in Norway spruce in relation to biotic and abiotic factors.

664      New Phytol 197:1173-1185.

665  Fan H, McGuire MA, Teskey RO (2017) Effects of stem size on stem respiration and its flux

666      components in yellow-poplar (*Liriodendron tulipifera* L.) trees. Tree Physiol 37:1536–

667      1545.

668  Ford CR, Wurzburger N, Hendrick RL, Teskey RO (2007) Soil DIC uptake and fixation in

669      *Pinus taeda* seedlings and its C contribution to plant tissues and ectomycorrhizal fungi.

670      Tree Physiol, 27:375-383.

671  Gartner BL, Moore JR, Gardiner BA (2004) Gas in stems: Abundance and potential

672      consequences for tree biomechanics. Tree Physiol 24:1239–1250.

673  Glavac V, Koenies H, Ebben U (1990) Seasonal variations in mineral concentrations in the

674      trunk xylem sap of beech (*Fagus sylvatica* L.) in a 42-year-old beech forest stand. New

675      Phytol 116:47-54.

676  Grossiord C, Mareschal L, Epron D (2012) Transpiration alters the contribution of

677      autotrophic and heterotrophic components of soil $CO_2$ efflux. New Phytol 194:647-653.

678  Hasselquist NJ, Metcalfe DB, Högberg P (2012) Contrasting effects of low and high nitrogen

679      additions on soil $CO_2$ flux components and ectomycorrhizal fungal sporocarp production

680      in a boreal forest. Global Change Biol 18:3596-3605.

681  Hilman B, Angert A (2016) Measuring the ratio of $CO_2$ efflux to $O_2$ influx in tree stem

682      respiration. Tree Physiol 36:1422-1431.

683  Hilman B, Muhr J, Trumbore SE, Kunert N, Carbone MS, Yuval P, Joseph Wright S, Moreno

684      G, Pérez-Priego O, Migliavacca M, Carrara A, Grünzweig JM, Osem Y, Weiner T, Angert

685      A (2019) Comparison of $CO_2$ and $O_2$ fluxes demonstrate retention of respired $CO_2$ in tree

686      stems from a range of tree species. Biogeosciences 16:177-191.

687     Hoch G, Richter A, Körner C (2003) Non-structural carbon compounds in temperate forest

688         trees. Plant, Cell and Environ 26:1067-1081.

689     Levy PE, Meir P, Allen SJ, Jarvis PG (1999) The effect of aqueous transport of $CO_2$ in xylem

690         sap on gas exchange in woody plants. Tree Physiol 19:53-58.

691     Lim H, Oren R, Palmroth S, Tor-ngern P, Mörling T, Näsholm T, Lundmark T, Helmisaari

692         H-S, Leppälammi-Kujansuu J; Linder S (2015) Inter-annual variability of precipitation

693         constrains the production response of boreal *Pinus sylvestris* to nitrogen fertilization.

694         Forest Ecol Manag 348:31-45.

695     Maier CA, Clinton BD (2006) Relationship between stem $CO_2$ efflux, stem sap velocity and

696         xylem $CO_2$ concentration in young loblolly pine trees. Plant Cell Environ 29:1471-1483.

697     Marshall JD, Cuntz M, Beyer M, Dubbert M,  Kuehnhammer K (2020) Borehole

698         equilibration: Testing a new method to monitor the isotopic composition of tree xylem

699         water in situ. Front Plant Sci 11:358.

700     Martin TA, Teskey RO, Dougherty PM (1994) Movement of respiratory $CO_2$ in stems of

701         loblolly pine (*Pinus taeda* L.) seedlings. Tree Physiol 14:481-495.

702     McGuire MA, Teskey RO (2002) Microelectrode technique for in situ measurement of

703         carbon dioxide concentrations in xylem sap of trees. Tree Physiol 22:807-811.

704     McGuire MA, Teskey RO (2004) Estimating tree stem respiration in trees by a mass balance

705         approach that accounts for internal and external fluxes of $CO_2$. Tree Physiol 24:571-578.

706     McGuire MA, Cerasoli S, Teskey RO (2007) $CO_2$ fluxes and respiration of branch segments

707         of sycamore (*Platanus occidentalis* L.) examined at different sap velocities, branch

708         diameters, and temperatures. J Exp Bot 58:2159-2168.

709     McGuire MA, Marshall JD, Teskey RO (2009) Assimilation of xylem-transported [13]C-

710         labelled $CO_2$ in leaves and branches of sycamore (*Platanus occidentalis* L.). J Exp Bot

711         60:3809-3817.

712    Negisi K (1979) Bark respiration rate in stem segments detached from young *Pinus*

713       *densiflora* trees in relation to velocity of artificial sap flow. J Jpn For Soc 61:88-93.

714    Perks MP, Irvine J, Grace J (2002) Canopy stomatal conductance and xylem sap abscisic acid

715       (ABA) in mature Scots pine during a gradually imposed drought. Tree Physiol 22:877-

716       883.

717    Pfanz H, Aschan G, Langenfeld-Heyser R, Wittmann C, Loose M (2002) Ecology and

718       ecophysiology of tree stems: corticular and wood photosynthesis. Naturwissenschaften

719       89:147-162.

720    Plaxton WC, Podestá FE (2006) The functional organization and control of plant respiration.

721       Crit Rev Plant Sci 25:159-198.

722    Powers EM, Marshall JD (2011) Pulse labeling of dissolved $^{13}$C-carbonate into tree xylem:

723       developing a method to determine the fate of recently fixed photosynthate. Rapid Comm

724       Mass Sp 25:33-40.

725    Salomón RL, Valbuena-Carabaña M, Teskey RO, McGuire MA, Aubrey D, González-

726       Doncel I, Gil L, Rodrìguez-Calcerrada J (2016) Seasonal and diel variation in xylem $CO_2$

727       concentration and sap pH in sub-Mediterranean oak stems. J Exp Bot 67:2817-2827.

728    Salomón RL, De Schepper V, Valbuena-Carabaña M, Gil L, Steppe K. (2018) Daytime

729       depression in temperature-normalised stem $CO_2$ efflux in young poplar trees is dominated

730       by low turgor pressure rather than by internal transport of respired $CO_2$. New Phytol

731       217:586-598.

732    Salomón RL, De Roo L, Bodé S, Boeckx P, Steppe K. (2019) Isotope ratio laser spectroscopy

733       to disentangle xylem-transported from locally respired $CO_2$ in stem $CO_2$ efflux. Tree

734       Physiol 39:819-830.

735    Saveyn A, Steppe K, Lemeur R (2007) Daytime depression in tree stem $CO_2$ efflux rates: Is it

736       caused by low stem turgor pressure? Ann Bot 99:477-485.

737    Saveyn A, Steppe K, McGuire MA, Lemeur R, Teskey RO (2008) Stem respiration and

738         carbon dioxide efflux of young *Populus deltoides* trees in relation to temperature and

739         xylem carbon dioxide concentration. Oecologia 154:637-649.

740    Sharp RG, Davies J (2009) Variability among species in the apoplastic pH signaling response

741         to drying soils. J Exp Bot 60:4363-4370.

742    Sorz J, Hietz P (2006) Gas diffusion through wood: implications for oxygen supply. Trees

743         20:34-41.

744    Steppe K, Saveyn A, McGuire MA, Lemeur R, Teskey RO (2007) Resistance to radial $CO_2$

745         diffusion contributes to between-tree variation in $CO_2$ efflux of *Populus deltoides* stems.

746         Funct Plant Biol 34:785-792.

747    Stockfors J, Linder S (1998) Effect of nitrogen on the seasonal course of growth and

748         maintenance respiration in stems of Norway spruce trees. Tree Physiol 18:155-166.

749    Stutz SS, Anderson J, Zulick R, Hanson DT (2017) Inside out: efflux of carbon dioxide from

750         leaves represents more than leaf metabolism. J Exp Bot 68:2849-2857.

751    Stutz SS, Hanson DT (2019) Contribution and consequences of xylem-transported $CO_2$

752         assimilation for $C_3$ plants. New Phytol 223:1230-1240.

753    Tarvainen L, Räntfors M, Wallin G (2014) Vertical gradients and seasonal variation in stem

754          $CO_2$ efflux within a Norway spruce stand. Tree Physiol 34:488-502.

755    Tarvainen L, Lutz M, Räntfors M, Näsholm T, Wallin G (2016) Increased needle nitrogen

756         contents did not improve shoot photosynthetic performance of mature nitrogen-poor Scots

757         pine trees. Front Plant Sci 7:1051.

758    Tarvainen L, Wallin G, Lim H, Linder S, Oren R, Ottosson Löfvenius M, Räntfors M, Tor-

759         ngern P, Marshall J (2018) Photosynthetic refixation varies along the stem and reduces

760         $CO_2$ efflux in mature boreal *Pinus sylvestris* trees. Tree Physiol 38:558-569.

761   Teskey RO, McGuire MA (2002) Carbon dioxide transport in xylem causes errors in

762      estimation of rates of respiration in stems and branches of trees. Plant Cell Environ

763      25:1571-1577.

764   Teskey RO, McGuire MA (2007) Measurement of stem respiration of sycamore (*Platanus*

765      *occidentalis* L.) trees involves internal and external fluxes of $CO_2$ and possible transport of

766      $CO_2$ from roots. Plant Cell Environ 30:570-579.

767   Teskey RO, Saveyn A, Steppe K, McGuire MA (2008) Origin, fate and significance of $CO_2$

768      in tree stems. New Phytol 177:17-32.

769   Thomas DS, Eamus D (2002) Seasonal patterns of xylem sap pH, xylem abscisic acid

770      concentration, leaf water potential and stomatal conductance of six evergreen and

771      deciduous Australian savanna tree species. Aust J Bot 50:229-236.

772   Tor-ngern P, Oren R, Oishi AC, Uebelherr JM, Palmroth S, Tarvainen L, Ottosson-Löfvenius

773      M, Linder S, Domec J-C, Näsholm T (2017) Ecophysiological variation of transpiration of

774      pine forests: synthesis of new and published results. Ecol Appl 27:118-133.

775   Trumbore SE, Angert A, Kunert N, Muhr J, Chambers JQ (2013) What's the flux?

776      Unraveling how $CO_2$ fluxes from trees reflect underlying physiological processes. New

777      Phytol 197:353-355.

778   Ubierna N, Kumar AS, Cernusak LA, Pangle RE, Gag PJ, Marshall JD (2009) Storage and

779      transpiration have negligible effects on C-13 of stem $CO_2$ efflux in large conifer trees.

780      Tree Physiol 29:1563-1574.

781   Usta I (2003) Comparative study of Wood desity by specific amount of void volume

782      (porosity). Turk J Agric For 27:1-6.

783   Vite JP, Rudinsky JA (1959) The water conducting systems in conifers and their importance

784      to the distribution of trunk injected chemicals. Contr. Boyce Thompson Inst. 20: 27-38.

785    Wallin G, Linder S, Lindroth A, Räntfors M, Flemberg S, Grelle A (2001) Carbon dioxide

786          exchange in Norway spruce at the shoot, tree and ecosystem scale. Tree Physiol 21:969-

787          976.

788    Werner RA, Bruch BA, Brand WA (1999) ConFlo III – An interface for high precision $\delta^{13}C$

789          and $\delta^{15}N$ analysis with an extended dynamic range. Rapid Comm Mass Sp 13:1237-1241.

790    Wittmann C, Pfanz H, Loreto F, Centritto M, Pietrini F, Alessio G (2006) Stem $CO_2$ release

791          under illumination: corticular photosynthesis, photorespiration or inhibition of

792          mitochondrial respiration? Plant Cell Environ 29:1149-1158.

793    Zelawski W, Riech FP, Stanley RG (1970) Assimilation and release of internal carbon

794          dioxide by woody plant shoots. Can J Bot 48:1351-1354.

795

1
2
3
4
5
6
7
8
9
10
11
12
13
14
15
16
17
18
19
20
21
22
23
24
25
26
27
28
29
30
31
32
33
34
35
36
37
38
39
40
41
42
43
44
45
46
47
48
49
50
51
52
53
54
55
56
57
58
59
60

796 **List of Figures**

797 **Figure 1** a) Stem temperature (°C) at 40 mm depth, and b) sap flow rates (l hr$^{-1}$) and above-

798 canopy photosynthetic photon flux density (PPFD, $\mu$mol m$^{-2}$ s$^{-1}$) between 16th of August and

799 13th of September 2014. Stem temperature and sap flow were measured at 1.5 m in the two

800 studied *Pinus sylvestris* trees. Solid lines: Tree 1; Dashed lines: Tree 2; in (b) upper half of

801 the sub-panel: PPFD. The dashed vertical lines indicate the start of the $^{13}$C label infusion on

802 the 22nd of August.

803

804 **Figure 2** Variation in observed $\delta^{13}$C efflux to a) the top of the canopy needle chambers, and

805 b-e) stem chambers along the boles of the two studied *Pinus sylvestris* trees. Solid lines: Tree

806 1; Dashed lines: Tree 2. The dashed vertical lines indicate the start of the $^{13}$C label infusion

807 on the 22nd of August. Note the change in y-axis scale among the sub-panels.

808

809 **Figure 3** Observed $^{13}$C enrichment ($\delta^{13}$C) of the xylem sap at 1.5 m (circles) and 5.3 m

810 (squares) in the two studied *Pinus sylvestris* trees. Filled symbols and solid lines: Tree 1;

811 Open symbols and dashed lines: Tree 2. Note the log-scaling of the y-axis. The dashed

812 vertical line indicates the start of $^{13}$C label infusion.

813

814 **Figure 4** Needle and phloem tissue $^{13}$C content following label infusion near the tree base on

815 the 22nd of August. Samples were collected on 27th of August (5 days after the labelling), 17th

816 of September (26 days after the labelling) and 22nd of September, phloem only (31 days after

817 the labelling). Filled symbols: Tree 1; Open symbols: Tree 2. The dashed vertical line

818 indicates the start of $^{13}$C label infusion.

819

820    **Figure 5** Number of days from the start of labelling until the maximum observed daily mean

821    $\delta^{13}C$ efflux along the boles of the two studied *Pinus sylvestris* trees. Filled symbols: Tree 1;

822    Open symbols: Tree 2. Regression line fitted to data pooled from both trees. The slope, 0.95

823    m day$^{-1}$, estimates the upward flux rate of xylem water in the stem.

**Table 1** $CO_2$ concentrations (%) of the xylem sap determined from samples collected 5, 10

and 13 days after the ^{13}C label insertion using equilibrium tubes at two heights along the

boles of the two studied *Pinus sylvestris* trees.

| Tree | Height (m) | 27 Aug | 1 Sep | 4 Sep |
|------|-----------|--------|-------|-------|
| 1 | 5.3 | 0.55 | 0.58 | n.a. |
|   | 1.5 | 0.11 | 0.71 | n.a. |
| 2 | 5.3 | 0.79 | 0.99 | 0.67 |
|   | 1.5 | 0.27 | 0.54 | 0.44 |

**Table 2** Carbon dioxide budgets of the 1.5 m to 5.3 m bole section in the two studied *Pinus sylvestris* trees calculated according to eq. 5. $E_c$ = observed net $CO_2$ efflux to the atmosphere, $A_R$ = corticular refixation of $CO_2$, $F_T$ = net sap $CO_2$ transport flux, and $R_s$ = total stem respiration (= $E_c + A_R + F_T$ with storage, $\Delta S$ in eq. 5, assumed negligible). All numbers for the $CO_2$ budget components are given as mol $CO_2$ m$^{-3}$ sapwood d$^{-1}$.

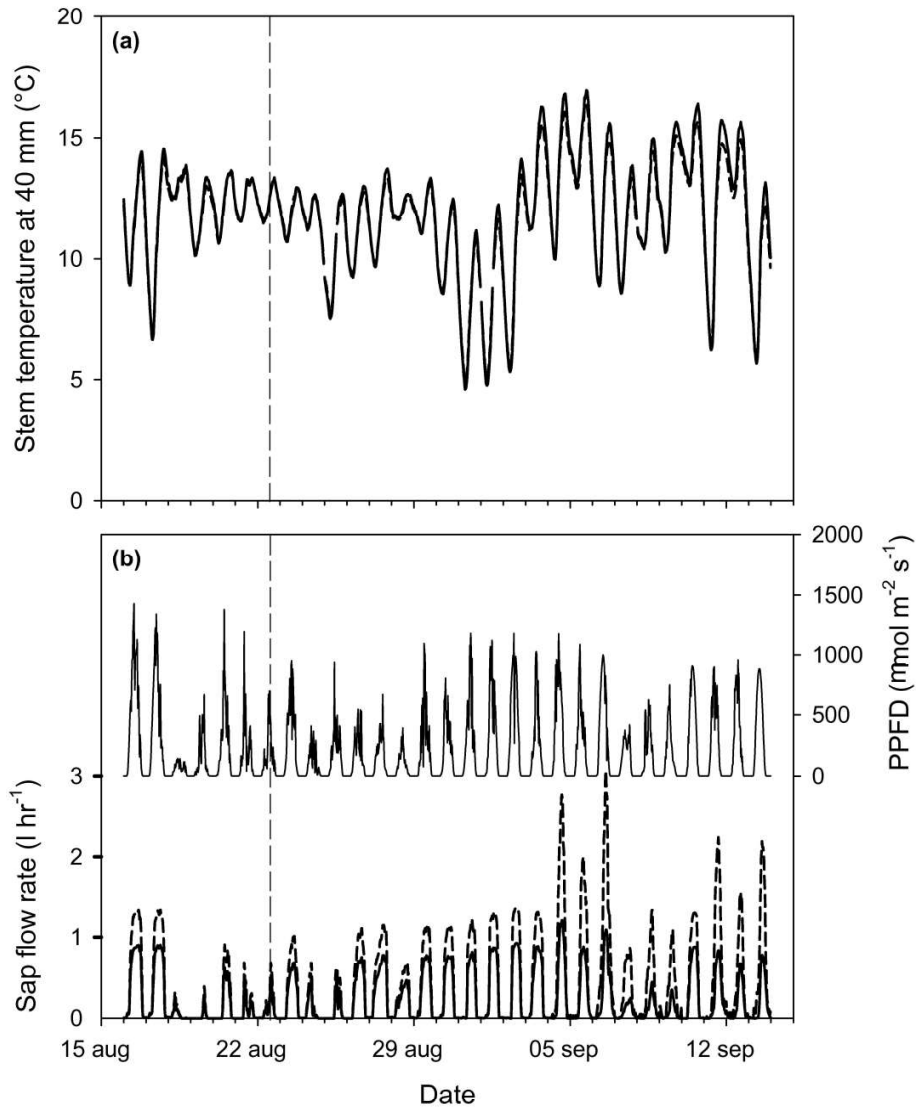| Tree | Date | $E_c$ | $A_R$ | $F_T$ | $R_S$ | $E_c/R_s$ (%) | $A_R/R_s$ (%) | $F_T/R_s$ (%) |
|---|---|---|---|---|---|---|---|---|
| 1 | 27 Aug | 1.15 | -0.14 | 0.06 | 1.07 | 107.3 | -12.8 | 5.5 |
| | 1 Sep | 0.78 | 0.03 | -0.02 | 0.79 | 98.2 | 4.1 | -2.3 |
| | 4 Sep | 0.97 | 0.16 | n.a. | n.a. | n.a. | n.a. | n.a. |
| 2 | 27 Aug | 1.84 | 0.12 | 0.08 | 2.04 | 90.3 | 5.8 | 3.8 |
| | 1 Sep | 1.39 | 0.17 | 0.07 | 1.63 | 85.5 | 10.3 | 4.2 |
| | 4 Sep | 2.00 | 0.19 | 0.05 | 2.24 | 89.2 | 8.6 | 2.0 |

Figure 1 a) Stem temperature (°C) at 40 mm depth, and b) sap flow rates (l hr-1) and above-canopy photosynthetic photon flux density (PPFD, µmol m-2 s-1) between 16th of August and 13th of September 2014. Stem temperature and sap flow were measured at 1.5 m in the two studied Pinus sylvestris trees. Solid lines: Tree 1; Dashed lines: Tree 2; in (b) upper half of the sub-panel: PPFD. The dashed vertical lines indicate the start of the 13C label infusion on the 22nd of August.
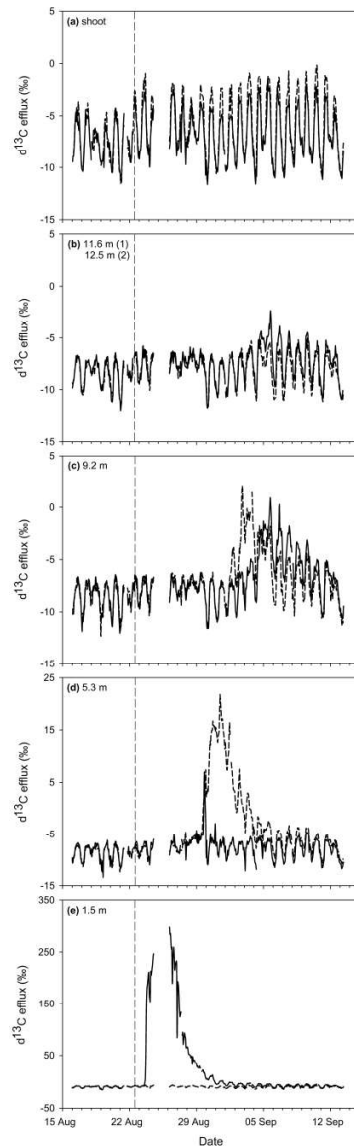
166x214mm (600 x 600 DPI)

1
2
3
4
5
6
7
8
9
10
11
12
13
14
15
16
17
18
19
20
21
22
23
24
25
26
27
28
29
30
31
32
33
34
35
36
37
38
39
40
41
42
43
44
45
46
47
48
49
50
51
52
53
54
55
56
57
58
59
60



Figure 2 Variation in observed δ13C efflux to a) the top of the canopy needle chambers, and b-e) stem chambers along the boles of the two studied Pinus sylvestris trees. Solid lines: Tree 1; Dashed lines: Tree 2. The dashed vertical lines indicate the start of the 13C label infusion on the 22nd of August. Note the change in y-axis scale among the sub-panels.
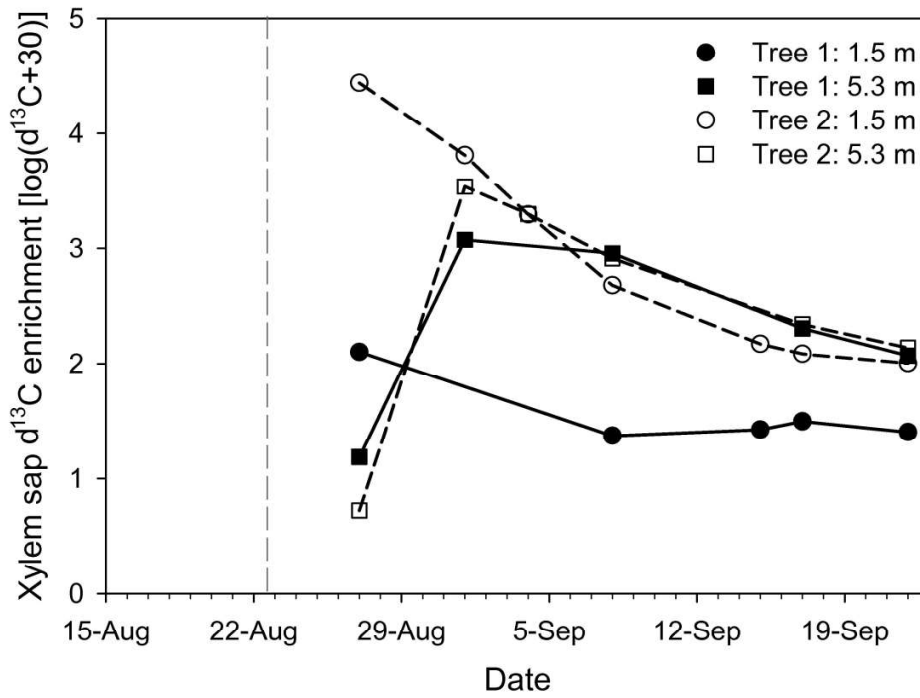
156x499mm (600 x 600 DPI)

1
2
3
4
5
6
7
8
9
10
11
12
13
14
15
16
17
18
19
20
21
22
23
24
25
26
27
28
29
30
31
32
33
34
35
36
37
38
39
40
41
42
43
44
45
46
47
48
49
50
51
52
53
54
55
56
57
58
59
60



Figure 3 Observed 13C enrichment (δ13C) of the xylem sap at 1.5 m (circles) and 5.3 m (squares) in the two studied Pinus sylvestris trees. Filled symbols and solid lines: Tree 1; Open symbols and dashed lines: Tree 2. Note the log-scaling of the y-axis. The dashed vertical line indicates the start of 13C label infusion.

150x119mm (600 x 600 DPI)

1
2
3
4
5
6
7
8
9
10
11
12
13
14
15
16
17
18
19
20
21
22
23
24
25
26
27
28
29
30
31
32
33
34
35
36
37
38
39
40
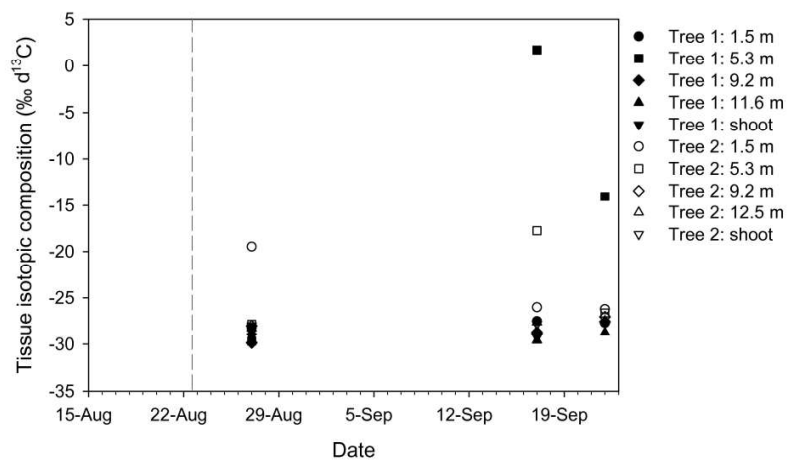41
42
43
44
45
46
47
48
49
50
51
52
53
54
55
56
57
58
59
60



Figure 4 Needle and phloem tissue 13C content following label infusion near the tree base on the 22nd of August. Samples were collected on 27th of August (5 days after the labelling), 17th of September (26 days after the labelling) and 22nd of September, phloem only (31 days after the labelling). Filled symbols: Tree 1; Open symbols: Tree 2. The dashed vertical line indicates the start of 13C label infusion.
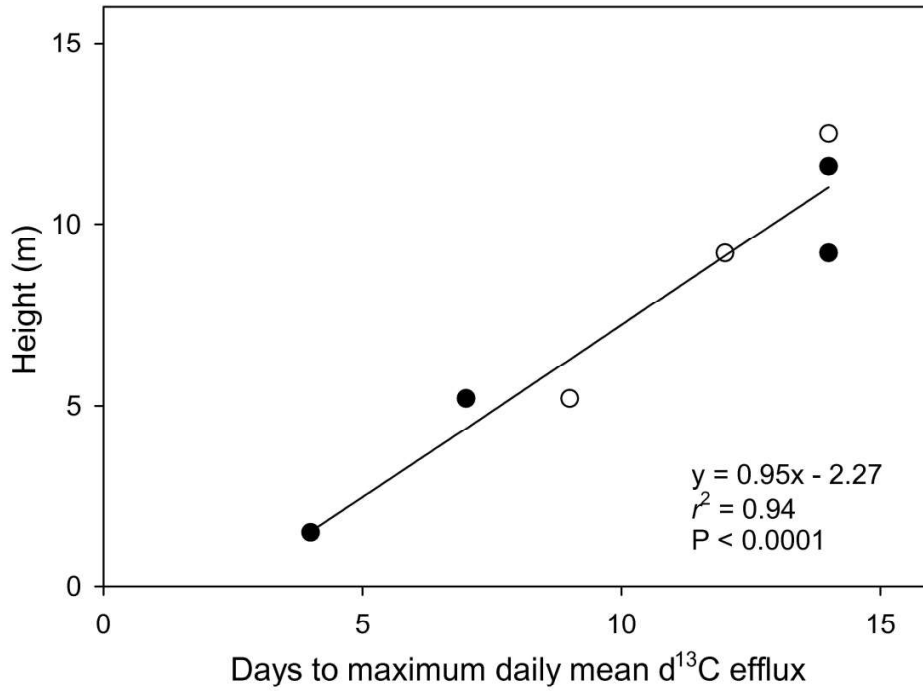
215x279mm (600 x 600 DPI)

1
2
3
4
5
6
7
8
9
10
11
12
13
14
15
16
17
18
19
20
21
22
23
24
25
26
27
28
29
30
31
32
33
34
35
36
37
38
39
40
41
42
43
44
45
46
47
48
49
50
51
52
53
54
55
56
57
58
59
60



Figure 5 Number of days from the start of labelling until the maximum observed daily mean δ13C efflux along the boles of the two studied Pinus sylvestris trees. Filled symbols: Tree 1; Open symbols: Tree 2. Regression line fitted to data pooled from both trees. The slope, 0.95 m day-1, estimates the upward flux rate of xylem water in the stem.

149x120mm (600 x 600 DPI)